Ian K.D. Pierce[1]

[1]Centre for the Observation and Modeling of Earthquakes, Volcanoes, and Tectonics, University of Oxford, UK

Corresponding author: Ian K.D. Pierce (ian@nevada.unr.edu)

Key Points

- Paleoseismic and lidar data are reevaluated to produce a paleoseismicity model for the Carson Range fault system in Nevada
- Results indicate five earthquakes occurred in this region during ~800-500 ybp.
- Previous seismic cycle ruptured a different combination of faults, highlighting variability of rupture segmentation

Abstract

At least five surface rupturing earthquakes that occurred during a <300 year time span near Carson City, Nevada form a spatiotemporal cluster of earthquakes similar to those observed on fault systems around the world. These earthquakes exhibit not only temporal clustering behavior, but also have varying rupture boundaries during successive earthquakes. The Carson Range Fault System is a series of east-dipping normal faults that extend ~100 km southwards from Reno, Nevada. Previously published paleoseismic and lidar data spanning this system provide evidence of six surface rupturing earthquakes that occurred across the Carson Range Fault System during the last 2500 years. The three most recent of these earthquakes occurred from 800-500 cal. ybp, and two other earthquakes occurred on the nearby Incline Village and East Carson Valley faults during this time period. Together these five M6.5-7.1 earthquakes form a spatiotemporal cluster or supercycle.

Plain Language Summary

Whether earthquakes occur randomly through time or exhibit clustering behavior is an important question for evaluating seismic hazards. Here I reanalyze nearly three decades worth of paleoseismic studies along the Carson Range Fault System near Reno, Nevada and Lake Tahoe to determine the past earthquake history of this region. The data reveal that a cluster of possibly five M6.5-7.1 earthquakes occurred during a 300 year time period roughly 800-500 years ago. This set of faults that ruptured during this cluster of earthquakes was quite different from those that ruptured during the previous earthquake cycle, approximately 2000-1500 years ago.

1 Introduction

Earthquakes across the spectrum of tectonic settings are increasingly recognized to frequently occur in temporal & spatial clusters, such as the Central Nevada Seismic Belt (Bell et al., 2004), the Central Apennines (Ferrarini et al., 2015), the Dasht-E Bayaz sequence of eastern Iran (Walker et al., 2004, 2011), the supercycles (e.g., Salditch et al., 2020) of the Alaskan, Chilean, Himalayan, Japanese, or Sumatran subduction zones (Sieh et al., 2008; Goldfinger et al., 2013; Herrendörfer et al., 2015; Wesnousky, 2020), or the cascading historical ruptures along the North and East Anatolian faults (Barka, 1996; Duman and Emre, 2013). In each of these examples, the time between earthquakes on neighboring faults or fault segments is much less than the average recurrence interval for each fault.

This temporal clustering of earthquakes is a time-dependent rupture behavior, as opposed to the poisson or time-independent rupture models that underpin most probabilistic seismic hazard assessment (PSHA) models (e.g., Field et al., 2014). In many cases coulomb stress changes (e.g., Stein et al., 1997; Scholz, 2010) alone are insufficient to explain these long duration sequences and that some viscoelastic relaxation process (Verdecchia et al., 2018; Salditch et al., 2020) is required to produce such spatiotemporal clusters over decadal or longer scales. Despite these challenges, the paucity of known historical clustering examples hampers our understanding of the mechanics and characteristics of this physical process. Recognition of prehistoric earthquake clusters can increase this catalogue, however often difficult-to-obtain detailed paleoseismic records are required to demonstrate the past occurrence of a cluster (Dolan et al., 2016; DuRoss et al., 2016). Here existing paleoseismic data are combined with geomorphic analyses of fault scarps along the length of the Carson Range Fault System in western Nevada to investigate possible clustering of late Holocene earthquakes.

This study examines how the overall Carson Range fault system (CRFS) behaves during ruptures, as whether individual fault segments rupture randomly through time, cluster temporally, or rupture together as large multifault ruptures is not well known. Constraining the paleoseismic history of this fault system is important for placing bounds on the size and frequency of earthquakes that pose significant seismic hazards to the Reno-Tahoe-Carson urban area, and for understanding what might control possible fault segmentation boundaries. Lidar data are used to produce a distribution of scarp vertical separation measurements along the entire fault system. The results of the numerous prior paleoseismic studies (gray dots in **Figure 1**) of individual fault segments along the CRFS are combined to investigate the overall rupture history of the fault system. These temporal data are then synthesized with the scarp distributions to determine the rupture length, displacement, magnitude, and timing of past earthquake ruptures. The result of this is a detailed paleoseismic history of the entire CRFS spanning the last two millennia.

1.1 Regional Setting

The Carson Range Fault System (CRFS) is located within the western Central Walker Lane, a ~100 km wide zone of distributed faults that together accommodate ~7 mm/yr of northwest directed dextral shear (e.g., Wesnousky, 2005; Wesnousky et al., 2012; Bormann et al., 2016; Pierce et al., 2021). The faulting within this region is generally composed of short (<50-km-long) discontinuous northwest striking dextral faults (e.g., Polaris fault; Hunter et al., 2011), northeast-striking sinistral faults (e.g., Carson lineament and Dog Valley fault; Li et al., 2017a), and north striking primarily normal faults (e.g., Antelope Valley, Smith Valley, Genoa, and West Tahoe faults; Ramelli et al., 1999; Kent et al., 2005; Sarmiento et al., 2011; Wesnousky and Caffee, 2011; Pierce et al., 2017) (**Figure 1**). GPS block models (e.g. Bormann et al., 2016) suggest that the faults along the Carson Range mostly accommodate extension, at a rate of ~0.6 mm/yr.

The CRFS is an east-dipping normal fault system extending from Reno, Nevada nearly 100 km southwards to near Markleeville, California (red faults in **Figure 1**). The CRFS spans the length of the Reno basin, Washoe Valley, and Carson Valley, and is composed of several different fault segments defined by surface fault traces and paleoseismic studies (**Figure 2a**). Lidar imagery reveal prominent and youthful fault scarps along the lengths of all the faults of the CRFS. The Genoa fault in Carson Valley (**Figure 1**) is the most studied fault of the CRFS (Ramelli et al., 1999; Ramelli and Bell, 2009; Rood et al., 2011; Wesnousky et al., 2016), and last produced an estimated ~M7 surface rupturing earthquake 515-421 cal. ybp. In Northern Carson Valley, near Carson City, the Genoa fault splays or branches into several faults (e.g. **Pierce et al., 2021**). North from Carson City are the subparallel Washoe Valley, Little Valley, and Mount Rose Fan Fault zones (e.g. Sarmiento et al., 2011).

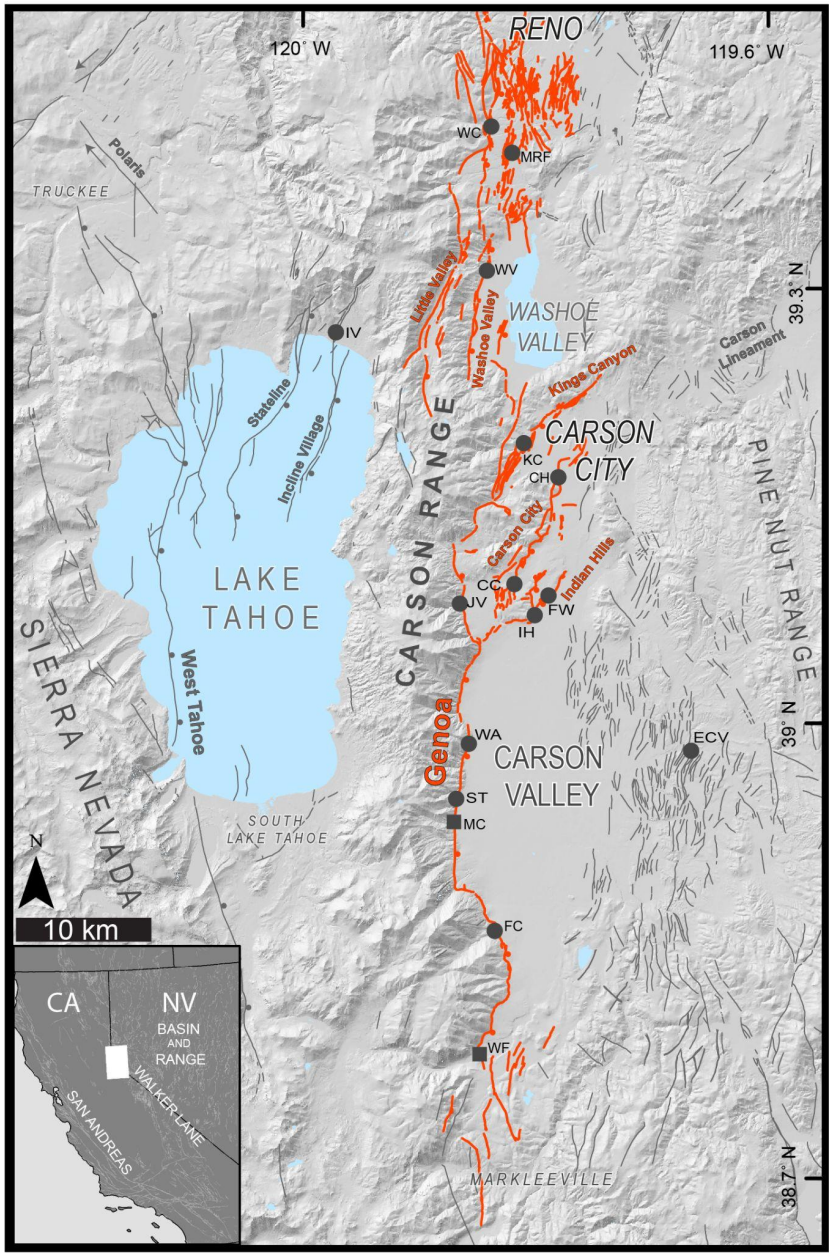

Figure 1 Overview map of the Carson Range Fault System (red) and surrounding region. Regional faults in gray (modified from USGS, 2020). Gray circles are prior trench sites and squares are slip rate sites. Abbreviations of past sites: ECV (East Carson Valley), WF (Woodfords), FC (Fay Canyon), MC (Mott Canyon), ST (Sturgis), WA (Walleys), IH (Indian Hills), FW (Freeway), JV (Jacks Valley), CC (Carson City), KC (Kings Canyon), CH (C-Hill),

WV (Washoe Valley), MRF (Mt. Rose Fan), WC (Whites Creek), IV (Incline Village).

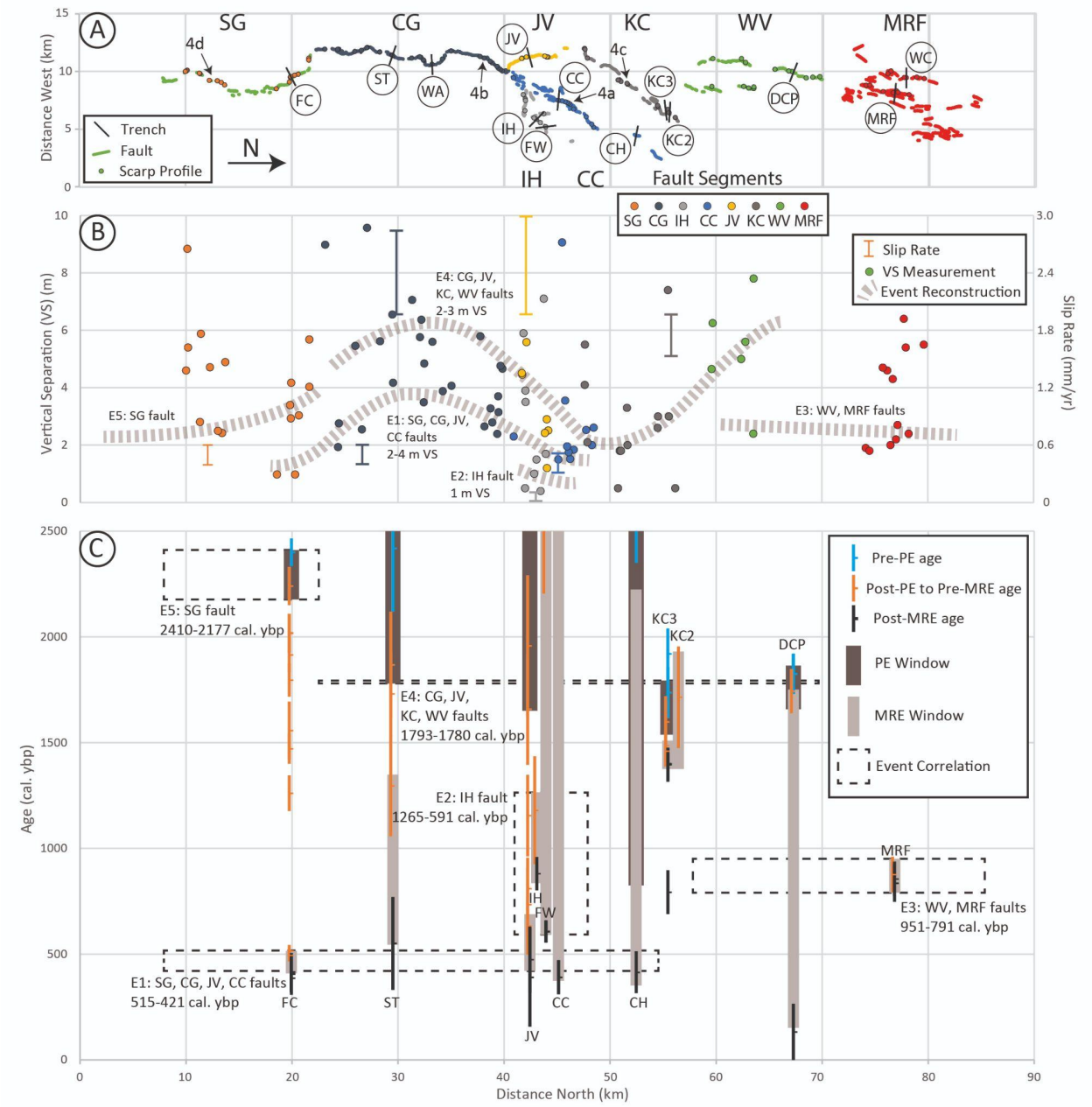

Figure 2 Space-time diagram of the Carson Range fault system. Fault names: SG: South Genoa; CG: Central Genoa; IH: Indian Hills; CC: Carson City; JV:

Jacks Valley; KC: Kings Canyon; WV: Washoe Valley; MRF: Mt Rose Fan; ECV: East Carson Valley, IV: Incline Village. (A) Map view plot of fault segments, vertical separation measurement locations, and trench sites. (B) plot of vertical separation measurements (dots, left axis) and slip rates (bars, right axis) against north distance, at the same scale as (A). Event reconstructions (dashed lines) are a hand-drawn estimate for illustration. (C) Plot of radiocarbon ages and OxCal modeled event horizons against north distance, at the same scale as (A) and (B). Radiocarbon ages are plotted as thin vertical bars showing the 95% uncertainty range with a horizontal tick at the midpoint of that range, and are colored as 3 groups based on each sample's relation to the Most Recent Event (MRE) and Penultimate Event (PE) event horizons. The thinner lighter gray vertical bars indicate the MRE horizon, while the slightly wider and darker gray bars are the PE horizon. The dashed black lines are event correlations between trenches, see text for description.

2 Distribution of Vertical Displacements along the Carson Range Fault System

Figure 2a shows the geographic locations of vertical separation (VS) measurements and trench sites along the CRFS (listed in **Table S3**). **Figure 2b** shows the distribution of VS measurements and slip rate estimates plotted along the fault system's average northerly strike. The resolution of available paleoseismic data is mostly limited to the two most recent earthquake cycles, which together produced <10 m of slip, so only VS measurements <10 m are plotted in **Figure 2b**. In general, the highest concentrations of larger VS measurements are along the Central Genoa, Jacks Valley, and Washoe Valley segments, ranging from ~3-7 m, while most VS measurements range from 1-5 m along the Southern Genoa, Carson City, Indian Hills, Kings Canyon, and Mt. Rose Fan segments. The cluster of ~3-6 m VS measurements near the 10 km mark are situated on a ~20 ka last glacial maxima outwash terrace (Rood et al., 2011; Wesnousky et al., 2016), which is at least ~15 ka older than most of the late Holocene surfaces along the rest of the range. Omitting these southernmost scarps leads to an overall bell-shaped distribution of offsets along the faults in Carson Valley. This result is consistent with not only topography, where the highest displacements are situated along the steepest sections of rangefront (**Figure 1**), but also with estimates of vertical slip rates (**Figure 2b**). The Southern Genoa fault near Woodfords has a late Pleistocene rate of 0.4-0.6 mm/yr (Rood et al., 2011; Wesnousky et al., 2016), the Central Genoa fault has a late Holocene rate of 2-3 mm/yr (Ramelli et al., 1999), the Kings Canyon fault has a Holocene rate of 1.5-2.0 mm/yr (dePolo, 2014), and the IH and CC faults have Holocene rates of <0.1 and ~0.4 mm/yr, respectively (**Pierce et al., 2021**) (**Figure 2b**).

At a given location along a fault, the smallest offsets are considered a result of the most recent earthquake, while larger offsets are the result of multiple events or simply larger displacements (e.g., Haddon et al., 2016; Li et al., 2017).

Following these rules, I attribute the cluster of ~2-3 m VS measurements near the -40 km mark on the Central Genoa and Jacks Valley segments to the MRE, while the ~5-6 m VS measurements are interpreted to be the result of the MRE and the penultimate event (**Figure 2b**). Thus, I interpret individual event distributions across the fault system, however relying on these displacement data alone leads to many possible interpretations. In the following section I combine these observations with the event timing data from prior paleoseismic studies to best fit both datasets.

The key observations in **Figure 2b** are the both (1) generally larger scarps and (2) wider range of scarp heights along the Genoa & Jacks Valley segments, compared to the smaller scarps that are more limited in their range of heights along the Kings Canyon, Indian Hills, and Carson City segments. This is attributed to be a result of distributed slip across these latter three northern segments, while all slip to the south is concentrated along the Genoa fault. This slip variation is proposed to be both a result of the frequency of earthquakes affecting each segment and the actual slip-per-event along each of these faults.

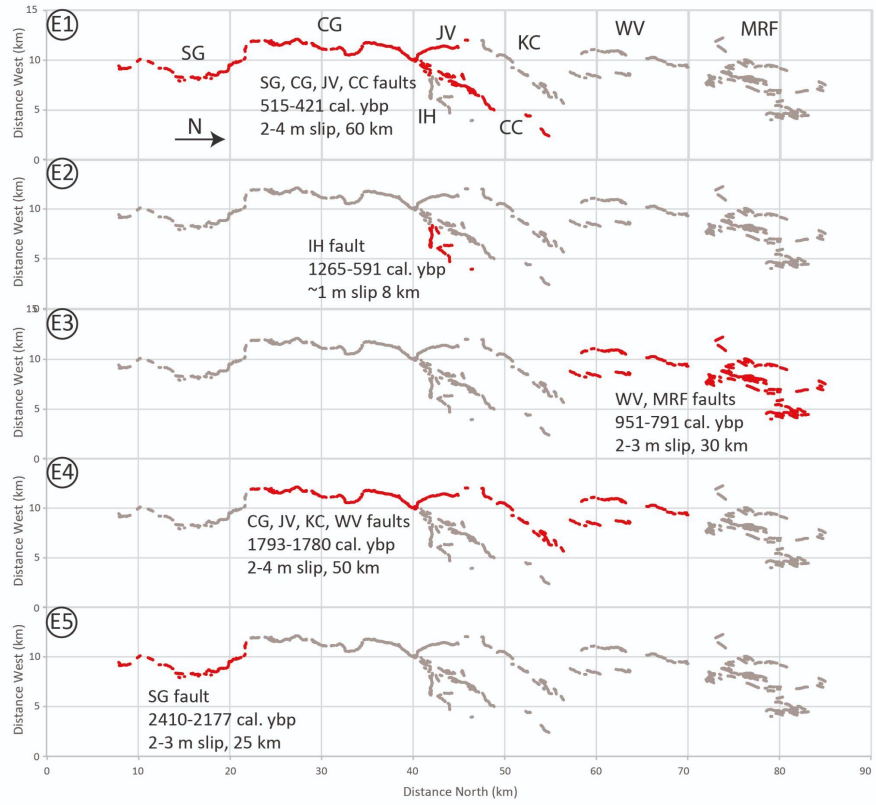

Figure 3 Reconstructed rupture history shows different fault segments rupturing in successive earthquakes.

3 Paleoseismicity of the Carson Range Fault System

To understand the timing of past events along the CRFS, the event horizons from prior trenching studies along the CRFS and surrounding faults were first collated (Ramelli and dePolo, 1996; Ramelli et al., 1999; Ramelli et al., 1999; dePolo and Sawyer, 2005; Ramelli et al., 2007; Ramelli and Bell, 2009; Sarmiento et al., 2011; Wesnousky and Caffee, 2011; dePolo, 2014; Seitz et al., 2016, Pierce et al., 2021). As these prior studies use a variety of different approaches for reporting and interpreting ages, their results were recalibrated using OxCal (Bronk Ramsey, 1995) to produce stratigraphic models bracketing event windows. I also reject two radiocarbon ages (IHR-1, ST-5) from this study, following the original investigators. The details of each past study are listed in the electronic supplement, and the resulting event windows for the most recent and penultimate events at each trench site are summarized in **Table S1**. The ages are plotted in the form of a space-time diagram in **Figure 2c**. Each trench site location is indicated on the schematic map of the faults (**Figure 2a**). The resulting constraints on event timing are not of sufficient resolution to differentiate whether ruptures of multiple faults were simultaneous during single larger magnitude events or if earthquakes occurred on neighboring faults over a period of time that could be as short as minutes (e.g., 1954 Dixie Valley/Fairview Peak sequence, Bell et al., 2004) or as long as several centuries, but for the following analyses are considered singular events if the event timing overlaps and the fault segments are adjacent. If a trench's event horizon overlaps with two adjacent trenches that have non-overlapping event windows, it is grouped with the younger of the two adjacent event windows. This approach is justified as in most cases the post-event limiting ages are from colluvial deposits that are assumed to be deposited rapidly following an earthquake (McCalpin, 2009), so events should be closer in time to the younger limiting ages.

Following this method results in an event model with 6 independent surface rupturing events across the CRFS during the past 2,500 years (**Figures 2 and 3, Table S2**). This paleoseismicity model is consistent with geomorphic observations bearing both on the recency and continuity of fault scarp character (**Figure 4**) and the vertical separation distribution (**Figure 2b**) from the lidar data. These ruptures have map lengths ranging from 8-60 km and displacements ranging from 1-4 m, corresponding to magnitudes M6.5-7.1 (**Figure 2b**). Events are numbered from most recent E1 to oldest E5. In this model, the most recent earthquake (E1) ruptured the entire Genoa fault and the Carson City fault (**Table S2, Figures 2 and 3**). The timing of this event is best bracketed by ages at the FC and JV sites, from 515-421 cal. ybp (**Figure 2c**). The displacement distribution from this event (**Figure 2b**) forms a clear bell shape for ~60 km, with ~3-4 m of vertical separation along the CG and JV segments, tapering to ~1-2 m along the SG and CC segments. E2 was a smaller event, occurring only on the 8-km-long IH fault, from 1265-591 cal. ybp. It is possible that E2 is actually E1, as interpreted by the original authors (Pierce

et al., 2021), but this requires rejecting two radiocarbon ages from fissure fills and the result does not significantly change the outcome of this study. E3 then occurred on the Washoe Valley and Mt. Rose Fan from 951-791 cal. ybp. E4* (not shown on **Figure 2**) ruptured the Kings Canyon fault. The next event, E4, ruptured the Central Genoa, Jacks Valley, Kings Canyon, and possibly Washoe Valley faults (**Figure 3**) from 1793-1780 cal. ybp. It is unknown if the E4 event continued northward into the Mt. Rose Fan. This event followed a similar slip distribution as E1, with ~3 m of VS on the CG and JV segments tapering to ~2-3 m along the KC and WV faults, for a total rupture length of ~50 km. The final event (E5) is only preserved in the FC trench but may have continued farther south towards Markleeville for a total length of ~25 km and occurred 2410-2177 cal. ybp (**Figures 1 and 2e**). It is unknown if E5 also ruptured the central part of the Genoa fault as the other trench records do not extend far enough back in time. Examples of scarps associated with E1, E4, and E5 of these ruptures are shown in **Figure 4**.

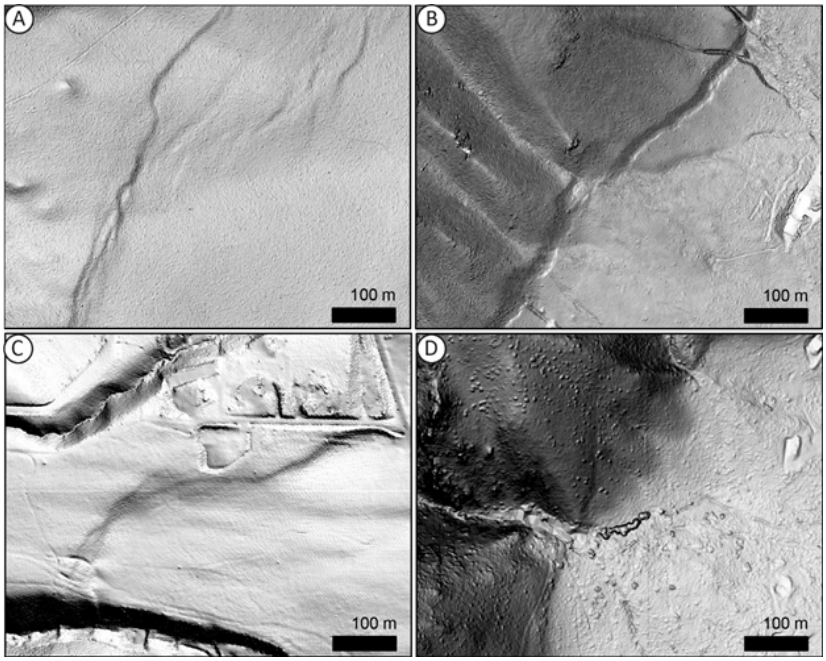

Figure 4 Lidar slope-shades of surface ruptures along various faults in the CRFS. Locations indicated on **Figure 2a**. (A) 1-2 m high single event fault scarps along Carson City fault resulting from E1 with fine well-preserved details of a complex stepover zone. (B) 2-3 m high single event fault scarps along the central Genoa fault resulting from E1 also have many well-preserved fine features and a clear graben preserved. (C) 3-7 m high multi-event fault scarps along the Kings Canyon fault zone resulting from E4 and earlier earthquakes. These scarps last ruptured ~1700 cal. ybp and still preserve many finer details.

(D) Degraded 2-5 m high multi-event fault scarps along the southernmost end of the Genoa fault have fewer fine details and no graben preservation compared to the other fault segments in this study. In my interpretation this part of the Genoa fault would have had <1 m of slip during E1 and therefore these scarps are mostly a result of E5 and possibly earlier earthquakes

4 Rupture boundaries, structural complexities, and event clustering

The most recent event, E1, ruptured the entire Genoa and Carson City faults. The penultimate event on the Genoa fault, E4, ruptured the central and northern parts of the Genoa fault, along with the Kings Canyon and possibly Washoe Valley faults. In this sense, the hills separating the Kings Canyon fault from the Jacks Valley fault form an earthquake gate (e.g., Duan et al., 2019; Liu et al., 2021), where the E1 rupture terminated, while the E4 rupture crossed this boundary. This alternating fault rupture pattern (**Figure 3**) provides an example of a fault system with non-persistent segment/rupture boundaries, that is, in subsequent events ruptures stopped at different points and ruptured different combinations of fault segments. This result suggests that it might be difficult to predict the endpoints of future ruptures, and that many possible rupture scenarios might be possible for a given fault system. DuRoss et al. (2016) found a similar variability of past rupture segmentation for the Wasatch fault in Utah.

Two other surface ruptures of nearby faults have also been shown to have occurred during the last millenia. In the eastern part of Carson Valley, the East Carson Fault (ECV) zone ruptured ~844-569 cal. ybp (**Figure 5a** and Table S1). In the Lake Tahoe basin, the Incline Village fault (IVF) ruptured ~600 cal. ybp (**Figure 5a,** Table S1). Taken together these five events (E1, E2, and E3, plus the IVF and ECV events) provide evidence of a prehistoric earthquake supercycle along the CRFS from ~500-800 cal. ybp. The individual recurrence times of each of these faults ranges from three to thirty times the 300 year length of this earthquake cluster, suggesting it is a non-random process, and represents a period of increased seismicity.

Similar earthquake clusters in normal faulting environments have been observed before in both the Central Apennines (**Figure 5a,** Ferrarini et al., 2015; Caporali et al., 2019) and the Walker Lane/Eastern California Shear Zone/Central Nevada Seismic Belt (**Figure 5b**, Bell et al., 2004). In both of these examples, major earthquakes "jump around" rather than forming a cascading or "unzipping" rupture pattern. These types of spatiotemporal clusters may migrate around the Basin and Range with time, rupturing a particular set of faults for a period of time before a different set of faults is activated. This implies that recent seismicity may significantly increase the probability of near-future seismicity for other nearby faults in a region, and that this elevated hazard may persist for a century or more. Similar to the 2016 Norcia sequence, my event

reconstruction also contains short single segment ruptures, responsible for clustering of ruptures over a short period of time. It is clear from both the Norcia sequence (Risi et al., 2016) and from modeling studies (Shin et al., 2014; Kostinakis and Morfidis, 2017) that successive moderate magnitude earthquakes can cause significantly more structural damage than single events. These observations highlight the importance that seismic hazard models not only account for large sources, but also for long periods of seismicity resulting from a variety of both small independent faults and larger sources.

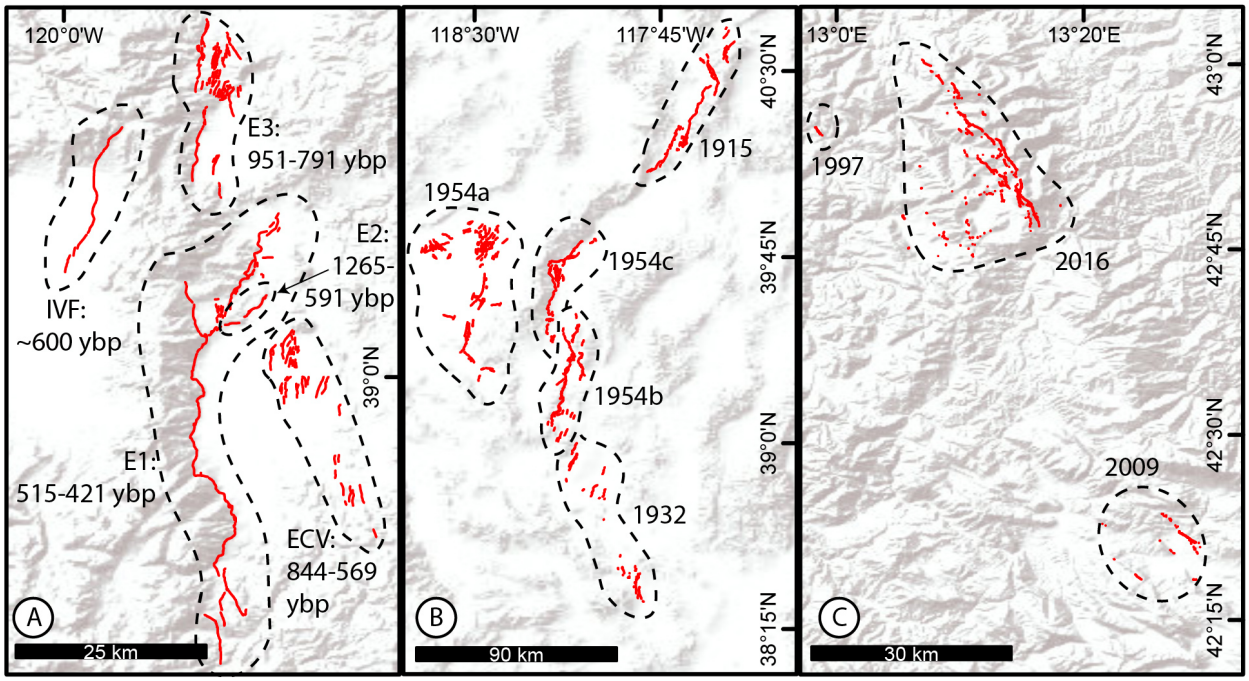

Fi

5 Examples of temporally clustered surface rupturing normal faults (red lines) in the region surrounding the CRFS (this study - A), Central Nevada Seismic Belt, USA (B), and Central Apennine, Italy (C). (B) 1915 M7.3 Pleasant Valley, 1932 M7.2 Cedar Mountain, 1954a 6.8 Rainbow Mountain & M6.6 Stillwater, 1954b M7.3 Fairview Peak, and 1954c M7.0 Dixie Valley earthquakes. Lines for (A) & (B) from USGS (2020). (C): 1997 M5.6 Colfiorito (lines from Pantosti et al., 1999), 2009 M6.1 L'Aquila (lines from Baize et al., 2020), and 2016 M6.0 Amatrice & M6.5 Norcia (lines Baize et al., 2020) earthquakes.

5 Conclusions

Combining the available paleoseismic data with lidar based observations of surface ruptures, demonstrates that the most recent event to have ruptured the Genoa and Carson City faults likely occurred ~515-421 cal. ybp, and produced 2-4 m of slip over 60 km, consistent with an ~M_w7 earthquake. During the

Genoa fault's penultimate surface rupturing earthquake ~1800 cal. ybp, the Carson City fault did not rupture, and instead the Kings Canyon fault ruptured, again producing an ~M_w7 earthquake with ~2-3 m of surface displacement. This provides a clear example of the variability of multisegment ruptures, with an alternating rupture pattern among major splay faults. In total, at least five surface rupturing earthquakes occurred during the period from ~800-500 cal. Ybp: one along the Genoa and Carson City faults in Carson Valley, a second smaller rupture along the Indian Hills fault near Carson City, a third in Washoe Valley and the Mt. Rose Fan, the fourth along the Incline Village fault, and a fifth on the Eastern Carson Valley fault. Together this series of earthquakes demonstrates that surface rupturing earthquakes in the Walker Lane have been spatially and temporally clustered in the past, which has important implications for our understanding of fault behavior and seismic hazards both in this region and globally.

Data Availability Statement

All paleoseismic data used are available in Electronic Supplement and are contained in the following references: Ramelli and dePolo (1996), Ramelli et al. (1999), Ramelli et al. (1999), dePolo and Sawyer (2005), Ramelli et al. (2007), Ramelli and Bell (2009), Sarmiento et al. (2011), Wesnousky and Caffee (2011), dePolo (2014), Seitz et al. (2016), and Pierce et al. (2021). Lidar data used for analysis are available by either contacting the US Army Corps of Engineers, Washoe County, or Douglas County, or for the USGS Reno Carson QL1 data only to registered US based researchers through OpenTopography.org.

Acknowledgements

Thank you to Gordon Seitz, Ramon Arrowsmith, Chris DuRoss, and Ben Johnson for discussions that helped to guide and improve this manuscript. Thanks to Paolo Boncio for a field trip to the 2016 Norcia ruptures inspiring me to finish this manuscript. Thanks also to Fiia Nurminen for digitizing the 1997 Colfiorito rupture. This work was supported by the Leverhulme Trust project 'EROICA'. There are no real or perceived financial or otherwise conflicts of interest.

References

Baize, S., Nurminen, F., Sarmiento, A., Dawson, T., Takao, M., Scotti, O., Azuma, T., Boncio, P., Champenois, J., Cinti, F.R., Civico, R., Costa, C., Guerrieri, L., Marti, E., McCalpin, J., Okumura, K., Villamor, P., 2020. A Worldwide and Unified Database of Surface Ruptures (SURE) for Fault Displacement Hazard Analyses. Seismol. Res. Lett. 91, 499–520. https://doi.org/10.1785/0220190144

Barka, A., 1996. Slip Distribution along the North Anatolian Fault Associated with the Large Earthquakes of the Period 1939 to 1967. Bull. Seismol. Soc.

Am. 86, 1238–1254.

Bell, J.W., Caskey, S.J., Ramelli, A.R., Guerrieri, L., 2004. Pattern and rates of faulting in the central Nevada seismic belt, and paleoseismic evidence for prior beltlike behavior. Bull. Seismol. Soc. Am. 94, 1229–1254.

Bormann, J.M., Hammond, W.C., Kreemer, C., Blewitt, G., 2016. Accommodation of missing shear strain in the Central Walker Lane, western North America: Constraints from dense GPS measurements. Earth Planet. Sci. Lett. 440, 169–177. https://doi.org/10.1016/j.epsl.2016.01.015

Bronk Ramsey, C., 1995. Radiocarbon Calibration and Analysis of Stratigraphy: The OxCal Program. Radiocarbon 37, 425–430. https://doi.org/10.1017/S0033822200030903

Caporali, A., Zurutuza, J., Bertocco, M., 2019. A Time-Dependent Model of Elastic Stress in the Central Apennines, Italy. J. Geophys. Res. Solid Earth 124, 9852–9869. https://doi.org/10.1029/2019JB017800

dePolo, C., 2014. Collaborative Research between the Nevada Bureau of Mines and Geology and the USGS on the Paleoearthquake History of the Kings Canyon Fault Zone, Nevada. USGS NEHRP.

dePolo, C.M., Sawyer, T., 2005. Paleoseismic studies along the Eastern Carson Valley fault system (Final Technical Report), U.S. Geological Survey National Hazards Reduction Program.

Dolan, J.F., McAuliffe, L.J., Rhodes, E.J., McGill, S.F., Zinke, R., 2016. Extreme multi-millennial slip rate variations on the Garlock fault, California: Strain super-cycles, potentially time-variable fault strength, and implications for system-level earthquake occurrence. Earth Planet. Sci. Lett. 446, 123–136. https://doi.org/10.1016/j.epsl.2016.04.011

Duan, B., Liu, Z., Elliott, A.J., 2019. Multicycle Dynamics of the Aksay Bend Along the Altyn Tagh Fault in Northwest China: 2. The Realistically Complex Fault Geometry. Tectonics 38, 1120–1137. https://doi.org/10.1029/2018TC005196

Duman, T.Y., Emre, Ö., 2013. The East Anatolian Fault: geometry, segmentation and jog characteristics. Geol. Soc. Lond. Spec. Publ. 372, 495–529. https://doi.org/10.1144/SP372.14

DuRoss, C.B., Personius, S.F., Crone, A.J., Olig, S.S., Hylland, M.D., Lund, W.R., Schwartz, D.P., 2016. Fault segmentation: New concepts from the Wasatch Fault Zone, Utah, USA. J. Geophys. Res. Solid Earth 121, 1131–1157. https://doi.org/10.1002/2015JB012519

Ferrarini, F., Lavecchia, G., de Nardis, R., Brozzetti, F., 2015. Fault Geometry and Active Stress from Earthquakes and Field Geology Data Analysis: The Colfiorito 1997 and L'Aquila 2009 Cases (Central Italy). Pure Appl. Geophys. 172, 1079–1103. https://doi.org/10.1007/s00024-014-0931-7

Field, E.H., Arrowsmith, R.J., Biasi, G.P., Bird, P., Dawson, T.E., Felzer, K.R., Jackson, D.D., Johnson, K.M., Jordan, T.H., Madden, C., Michael, A.J., Mil-

ner, K.R., Page, M.T., Parsons, T., Powers, P.M., Shaw, B.E., Thatcher, W.R., Weldon, R.J., Zeng, Y., 2014. Uniform California Earthquake Rupture Forecast, Version 3 (UCERF3)—The Time-Independent ModelUniform California Earthquake Rupture Forecast, Version 3 (UCERF3)—The Time-Independent Model. Bull. Seismol. Soc. Am. 104, 1122–1180. https://doi.org/10.1785/0120130164

Goldfinger, C., Ikeda, Y., Yeats, R.S., Ren, J., 2013. Superquakes and Supercycles. Seismol. Res. Lett. 84, 24–32. https://doi.org/10.1785/0220110135

Herrendörfer, R., van Dinther, Y., Gerya, T., Dalguer, L.A., 2015. Earthquake supercycle in subduction zones controlled by the width of the seismogenic zone. Nat. Geosci. 8, 471–474. https://doi.org/10.1038/ngeo2427

Hunter, L.E., Howle, J.F., Rose, R.S., Bawden, G.W., 2011. LiDAR-Assisted Identification of an Active Fault near Truckee, California. Bull. Seismol. Soc. Am. 101, 1162–1181. https://doi.org/10.1785/0120090261

Kent, G.M., Babcock, J.M., Driscoll, N.W., Harding, A.J., Dingler, J.A., Seitz, G.G., Gardner, J.V., Mayer, L.A., Goldman, C.R., Heyvaert, A.C., Richards, R.C., Karlin, R., Morgan, C.W., Gayes, P.T., Owen, L.A., 2005. 60 k.y. record of extension across the western boundary of the Basin and Range province: Estimate of slip rates from offset shoreline terraces and a catastrophic slide beneath Lake Tahoe. Geology 33, 365–368. https://doi.org/10.1130/G21230.1

Kostinakis, K., Morfidis, K., 2017. The impact of successive earthquakes on the seismic damage of multistorey 3D R/C buildings. Earthq. Struct. 12, 1–12. https://doi.org/10.12989/eas.2017.12.1.001

Li, X., Huang, W., Pierce, I.K.D., Angster, S.J., Wesnousky, S.G., 2017. Characterizing the Quaternary expression of active faulting along the Olinghouse, Carson, and Wabuska lineaments of the Walker Lane. Geosphere 13, 2119–2136. https://doi.org/10.1130/GES01483.1

Liu, D., Duan, B., Prush, V.B., Oskin, M.E., Liu-Zeng, J., 2021. Observation-constrained multicycle dynamic models of the Pingding Shan earthquake gate along the Altyn Tagh Fault. Tectonophysics 814, 228948. https://doi.org/10.1016/j.tecto.2021.228948

McCalpin, J., 2009. Paleoseismology, 2nd ed. Academic Press.

Pantosti, D., De Martini, P.M., Galli, P., Galadini, F., Messina, P., Moro, M., Sposato, A., 1999. Studi Paleosismologici Attraverso La Rottura Superficiale Prodotta Dal Terremoto Del 14 Ottobre 1997 (Umbria-Marche). Atti 18° Convegno Naz. 10.07.

Pierce, I.K.D., Wesnousky, S.G., Owen, L.A., 2017. Terrestrial cosmogenic surface exposure dating of moraines at Lake Tahoe in the Sierra Nevada of California and slip rate estimate for the West Tahoe Fault. Geomorphology 298, 63–71. https://doi.org/10.1016/j.geomorph.2017.09.030

Pierce, I.K.D., Wesnousky, S.G., Owen, L.A., Bormann, J.M., Li, X.,

Caffee, M., 2021. Accommodation of Plate Motion in an Incipient Strike-Slip System: The Central Walker Lane. Tectonics 40, e2019TC005612. https://doi.org/10.1029/2019TC005612

Ramelli, A.R., Bell, J.W., 2009. Spatial and Temporal Patterns of Fault Slip Rates on the Genoa Fault. USGS NEHRP.

Ramelli, Alan R., Bell, J.W., dePolo, C.M., Yount, J.C., 1999. Large-magnitude, late Holocene earthquakes on the Genoa fault, west-central Nevada and eastern California. Bull. Seismol. Soc. Am. 89, 1458–1472.

Ramelli, A.R., dePolo, C.M., 1996. Trenching and Related Studies of the Northern Sierra Nevada Range-front Fault System. USGS NEHRP.

Ramelli, A.R., dePolo, C.M., Bell, J.W., 2007. Paleoseismic studies of the Little Valley fault. USGS NEHRP.

Ramelli, A.R., dePolo, C.M., Bell, J.W., 1999. Paleoseismic studies of the Northern Sierra Nevada frontal fault zone (Final Technical Report), U.S. Geological Survey National Earthquake Hazards Reduction Program.

Risi, R.D., Sextos, A., Zimmaro, P., Simonelli, A., Stewart, J., 2016. THE 2016 CENTRAL ITALY EARTHQUAKE SEQUENCE: OBSERVATIONS OF INCREMENTAL BUILDING DAMAGE. Los Angel. 12.

Rood, D.H., Burbank, D.W., Finkel, R.C., 2011. Spatiotemporal patterns of fault slip rates across the Central Sierra Nevada frontal fault zone. Earth Planet. Sci. Lett. 301, 457–468. https://doi.org/10.1016/j.epsl.2010.11.006

Salditch, L., Stein, S., Neely, J., Spencer, B.D., Brooks, E.M., Agnon, A., Liu, M., 2020. Earthquake supercycles and Long-Term Fault Memory. Tectonophysics 774, 228289. https://doi.org/10.1016/j.tecto.2019.228289

Sarmiento, A.C., Wesnousky, S.G., Bormann, J.M., 2011. Paleoseismic Trenches across the Sierra Nevada and Carson Range Fronts in Antelope Valley, California, and Reno, Nevada. Bull. Seismol. Soc. Am. 101, 2542–2549. https://doi.org/10.1785/0120100176

Scholz, C.H., 2010. Large Earthquake Triggering, Clustering, and the Synchronization of Faults. Bull. Seismol. Soc. Am. 100, 901–909. https://doi.org/10.1785/0120090309

Seitz, G., Kent, G., Driscoll, N., Dingler, J., 2016. Large Earthquakes on the Incline Village Fault from Onshore and Offshore Paleoseismology, Lake Tahoe, California-Nevada, in: Applied Geology in California, AEG Special Publications. p. 1000.

Shin, J., Kim, J., Lee, K., 2014. Seismic assessment of damaged piloti-type RC building subjected to successive earthquakes. Earthq. Eng. Struct. Dyn. 43, 1603–1619. https://doi.org/10.1002/eqe.2412

Sieh, K., Natawidjaja, D.H., Meltzner, A.J., Shen, C.-C., Cheng, H., Li, K.-S., Suwargadi, B.W., Galetzka, J., Philibosian, B., Edwards, R.L., 2008. Earthquake Supercycles Inferred from Sea-Level Changes Recorded in the Corals of West Sumatra. Science 322, 1674–1678. https://doi.org/10.1126/science.1163589

Stein, R.S., Barka, A.A., Dieterich, J.H., 1997. Progressive failure on the North Anatolian fault since 1939 by earthquake stress triggering. Geophys. J. Int. 128, 594–604. https://doi.org/10.1111/j.1365-246X.1997.tb05321.x

USGS, 2020. U.S. Geological Survey Quaternary fault and fold database for the United States.

Verdecchia, A., Pace, B., Visini, F., Scotti, O., Peruzza, L., Benedetti, L., 2018. The Role of Viscoelastic Stress Transfer in Long-Term Earthquake Cascades: Insights After the Central Italy 2016–2017 Seismic Sequence. Tectonics 37, 3411–3428. https://doi.org/10.1029/2018TC005110

Wesnousky, S.G., 2020. Great Pending Himalaya Earthquakes 9.

Wesnousky, S.G., 2005. Active faulting in the Walker Lane. Tectonics 24, 35 pp. https://doi.org/10.1029/2004TC001645

Wesnousky, S.G., Aranguren, R., Rengifo, M., Owen, L.A., Caffee, M.W., Murari, M.K., Pérez, O.J., 2012. Toward quantifying geomorphic rates of crustal displacement, landscape development, and the age of glaciation in the Venezuelan Andes. Geomorphology 141–142, 99–113. https://doi.org/10.1016/j.geomorph.2011.12.028

Wesnousky, S.G., Briggs, R.W., Caffee, M.W., Ryerson, F.J., Finkel, R.C., Owen, L.A., 2016. Terrestrial cosmogenic surface exposure dating of glacial and associated landforms in the Ruby Mountains-East Humboldt Range of central Nevada and along the northeastern flank of the Sierra Nevada. Geomorphology 268, 72–81. https://doi.org/10.1016/j.geomorph.2016.04.027

Wesnousky, S.G., Caffee, M., 2011. Range-Bounding Normal Fault of Smith Valley, Nevada: Limits on Age of Last Surface-Rupture Earthquake and Late Pleistocene Rate of Displacement. Bull. Seismol. Soc. Am. 101, 1431–1437. https://doi.org/10.1785/0120100238